Research Article – Vol. 02, Issue 02, No. 03

Bilijipublication

Advanced in Engineering and Intelligence Systems

Journal Web Page: https://aeis.bilijipub.com

Pressure Reduction Effects of Compressible Materials on The Buried Pipes Subjected to Large Surcharges

Marcin Kochanowicz[1], Vo Van Hoang[2,*]

[1] *Faculty of Electrical Engineering, Bialystok University of Technology, Wiejska 45C, 15-531, Bialystok, Poland*
[2] *Vietnam National University, Ho Chi Minh City, Vietnam*

Highlights

- Compressible materials used to mitigate pressure effects in geotechnical applications.
- Induced Trench Installation (ITI) method reduces pressure on buried pipes by installing a compressible zone.
- Study investigates the efficiency of EPS geofoam configurations on buried pipe performance under surcharge.
- Numerical analysis shows significant impact of geofoam block stiffness on the mechanical response.
- Improper arrangement of compressible materials can lead to excessive axial force and bending moment, negatively affecting pipe performance.

Article Info

Received: 08 February 2023
Received in revised: 25 April 2023
Accepted: 25 April 2023
Available online: 28 June 2023

Keywords

ITI,
buried pipe,
transferred pressure,
numerical analysis,
surcharge pressure;

Abstract

Compressible materials including Expanded Polystyrene (EPS) blocks have been extensively used in many geotechnical applications to reduce the effects of applied pressure. Of particular concern where a high embankment is placed above a buried pipe, excessive deformation and stresses may be developed in the pipe walls. The induced Trench Installation (ITI) method could be used as an alternative to mitigate the transferred pressure to the buried structure. In this method, a compressible zone is installed above the buried pipe to induce positive soil arching and subsequently reduce applied pressure to the pipe. This study aims to investigate the efficiency of the various configuration of EPS geofoam (as compressible material) on the performance of the buried pipe subjected to a large surcharge. Two-dimensional numerical analyses were conducted considering the incrementally increasing pressure applied on the surface of dry sand containing buried pipe. The analysis results were compared to the no EPS state to present the effectiveness of different EPS arrangements. It was concluded that the stiffness of geofoam blocks significantly affects the mechanical response of buried structure. Furthermore, applying compressible materials with a specific array leads to the development of excessive axial force and bending moment in the pipe wall and has adverse effects on the pipe performance.

1. Introduction

To design buried structures, it is necessary to predict the magnitude of transferred pressure. Where the structure is placed beneath high embankments, buried conduits experience high values of pressure which necessitate careful determination of developed forces and bending moments in pipe skin to yield an appropriate design [1]. The performance of a structure subjected to the surrounded soil pressure is known to be influenced by the geometry of the pipe, installation method, and backfill properties [2-6]. So far, many techniques have been proposed to reduce applied pressure on the buried structures including the application of geotextiles and geogrids, bridging method, installation of pipe within soft materials, inclusion of compressible materials above the structure, etc. [7-12]. Marston [13, 14] pioneered research for mitigation of

* Corresponding Author: Vo Van Hoang
Email: vvhoang@inu.edu.vn

transferred pressure to the buried structure by applying a soft zone above the pipe. The induced trench installation (ITI) method involves excavating a trench around an existing buried structure, installing compressible materials such as EPS geofoam blocks in the trench, and then backfilling with soil. The purpose of this method is to reduce transferred pressure from external loads by creating a zone of low stiffness or modulus around the buried structure [15]. When loads are applied on top of soil containing an ITI system, they cause stresses within the soil mass which may lead to deformation and redistribution of stresses around buried structures like pipes or culverts. In some cases, this can result in stress concentrations being reduced due to arching effects created by compressible materials used in ITI systems. By reducing transferred pressure through use of compressible materials like EPS geofoam blocks installed using an ITI approach can help mitigate excessive deformation and stresses within pipe walls subjected to large surcharges [16]. Marston's study was followed by Spangler [17, 18] and ultimately led to the presentation of Marston-Spangler theory. Although soft materials like sawdust and low-density sand soil could be used as a soft zone in this technique of installation [19], the provision of Expanded Polystyrene (EPS) geofoams is a perfect alternative. EPS is a lightweight, rigid plastic foam insulation material produced from solid beads of polystyrene. The production process involves expanding these beads with steam and then molding them into various shapes and sizes for different applications. EPS has low thermal conductivity, high compressive strength, good shock absorption properties, and is resistant to moisture damage [20]. This material could be regarded as cost-effective, easy to transport, easy to apply, and environment-friendly [21, 22].

When the buried structure undergoes large pressures induced by soil weight and probable traffic loads at the ground surface, the geofoam buffer above the pipe compresses and subsequently the soil column above that settles more than adjacent soil columns. The relative displacement between these columns led to positive soil arching mobilization and reduced pressure on the buried structure crest. The reported benefits of ITI technique can be traced back to the studies since the early twentieth century. While the small-scale and numerical analyses are widely used in geotechnical applications [23-26], the soil-structure interaction and overall concept of the ITI method have also been investigated by laboratory tests [27, 28], field measurements [29-31], and numerical analyses [32-37]. The main outcome of these earlier works is the recognition that compressible materials like EPS can be effective in mitigating excessive deformation and stresses on buried structures subjected to high embankments or surcharges. Naderi et al [38] found that using a layer of EPS blocks above a buried pipe reduced vertical stress on the pipe's crown and increased soil arching effects, resulting in lower maximum bending moments compared to an unimproved case. A study noted that using EPS blocks as a compressible layer beneath a rigid pavement reduced vertical stresses on underlying soil layers and improved overall pavement performance under heavy traffic loads [39].

The geometry of EPS buffer is characterized by width, thickness, and gap distance between geofoam and crest of the buried structure. Kim and Yoo [33] studied the role of geofoam thickness in mitigating applied pressure. Yoo and Kang [40] noted the effectiveness of EPS cover around the buried pipe in reducing transferred stresses. The laboratory tests performed by Meguid et al. [41] aimed to examine the influence of box culvert wrapping by geofoam sheets on the response of a buried structure. However, little is known about the efficiency of different arrangements of EPS geofoam on the performance of pipes buried within backfills subjected to immense applied surface pressure.

This study specifically focuses on investigating the efficiency of different configurations of EPS geofoam on buried pipes subjected to large surcharges. The research aims to compare their analysis results with a no-EPS state and present the effectiveness of various EPS arrangements. To this end, a series of numerical analyses will be developed after validation of numerical modeling by well-documented experimental results. The performance of the buried pipe is judged by the pipe wall's developed axial forces and bending moments. In addition, the profile of ground settlement will be studied in models with different geofoam arrangements. As the stiffness of EPS buffer plays a vital role in pipe response, particular attention has also been dedicated to this factor.

2. Numerical Modeling

Modeling buried conduits within soil medium need an appropriate selection of constitutive models and choosing suitable soil-pipe and soil-geofoam contact behavior. While advanced models for simulation of soil behavior in many geotechnical applications were reported to yield the more fitted results to the analytical and experimental outcomes, the traditional mohr-coulomb model has been found suitable for investigating buried culvert performance [42-44]. Moreover, it has been found by many researchers that EPS shows a nonlinear response under uniaxial and triaxial loading; however, in small strain conditions like the state of geofoam included above the buried pipe, simple linear behavior appropriately could be adopted [31, 45-47]. Thus,

elastic-plastic mohr-coulomb and linear elastic models were chosen for response simulation of backfill and geofoam inclusion for the numerical modeling of this study. The PLAXIS 2D CE [48] was employed to conduct FE analyses. This program can simulate soil-structure interaction and presents a wide variety of model to simulate soil and structure behavior, making it popular in geotechnical analyses [24, 49]. The 15-noded triangular plane strain elements are used to mesh backfill soil and EPS isolations while the buried structure is meshed using linear plate elements of the PLAXIS library. The interaction of soil-pipe and soil-geofoam has been simulated using interface elements that allow slippage and separation of mediums in contact. For soil-pipe and soil-geofoam, the value of R_{int} is introduced to the program. By definition, the R_{int} relates the interface friction φ_{int} to the strength parameters of backfill soil φ_s ($R_{int} = \tan(\varphi_{int}) / \tan(\varphi_s)$). The Mohr-culoumb interface algorithm is used to simulate and analyze interactions between different materials or layers within a soil structure in PLAXIS [50]. This algorithm considers sliding along interfaces between layers or materials with different properties (such as stiffness or shear strength), separation due to tensile stresses and contact forces due to compression.

To achieve the purpose of this study, it is required to validate numerical modeling with measured data in the literature. Accordingly, numerical modeling will be developed to investigate the performance of buried conduits with EPS different arrangements.

3. Verification of Numerical Model

For verification, the experimental results of Ahmed [51] study were found to be well-documented research with a detailed description of conducted small-scale experiments and a complete description of used material. The researcher assessed the effect of EPS buffer on the transferred pressure to buried box culverts. The test was performed by placing a 0.25×0.25 m square box profile with 10 mm thickness within a 140×120×0.45 m (length×height×width) test box. The container was backfilled by dry sandy gravel to the height of one meter while the buried box was overlain by 5 cm thick EPS geofoam, with a density of 14.4 kg/m^3 (EPS15) to simulate induced trench installation (ITI) method. Elastic modulus (E), poisson's ratio (ν), friction angle (φ'), and dilation angle (ψ) of backfill soil is reported as 150 MPa, 0.3, 47°, and 15°, respectively. 4.2 MPa and 0.1 were also adopted as elastic modulus and poisson's ratio of EPS15. For comparison, a test without EPS geofoam was also considered, the result of which is presented as NO EPS state. Surface pressure was incrementally increased to the maximum of 140 kPa at the surface of the backfill material by using a pressurized air bladder. Friction coefficient (μ=tanφ) of soil-EPS, soil-culvert, and EPS-culvert is respectively chosen equal to 0.6, 0.45, and 0.3 per provided data by Meguid and Hussein [52]. Conducted tests aimed to examine the transferred pressure to the buried culvert with and without EPS inclusion. The buried hollow box was instrumented using tactile pressure meters to record contact pressure on the culvert's top, side, and bottom wall caused by applied surface pressure. A full description of the test procedure, instrumentation, and outcome can be found in [51]. The general view of test box components along with their finite element meshing is represented in **Error! Reference s ource not found.**. The location of boundaries has ensured through a try-and-error process by modeling various geometries and choosing the boundaries far enough from the studied area to avoid the adverse effect of boundaries on the stress and deformation pattern of the soil medium.

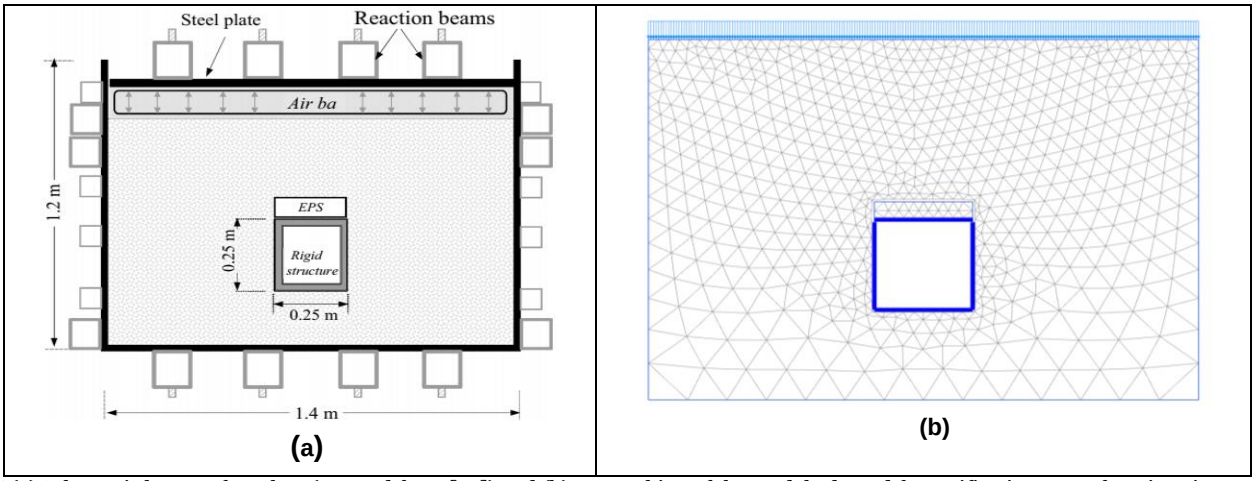

Fig. 1. DG(a) Schematic layout of test box (sourced from [52]) and (b) FE meshing of the model adopted for verification curve functions in terms of their nominal powe

Fig. **2.** Comparison of measured and calculated average applied pressure on the top wall of the buried box in the model (a) without EPS and (b) with EPS15 inclusion

illustrates the results of numerical analyses and instrumental readings of contact pressure transferred to the culvert upper wall. Due to the ununiform distribution of contact pressure on culvert walls as demonstrated by [8, 53, 54], the data in the figure represent the mean values of the computed and measured pressure. As shown, numerical results are well fitted to the experimental data presented in the original reference. In the No EPS model, there are some differences between readings and computed with the maximum of less than 20% when applied surface pressure is about 76 kPa. However, the ultimate values (at the surface pressure of 140 kPa) are closely matched. From the curves shown in Fig. **2.** Comparison of measured and calculated average applied pressure on the top wall of the buried box in the model (a) without EPS and (b) with EPS15 inclusion

, it could be perceived that the inclusion of geofoam block immediately above the buried box culvert, significantly reduced the contact pressure of the upper wall from 152.62 kPa to 44.73 kPa. It should be noted that the computed linearly increased transferred pressure is also observed through many studies [29, 55-57]. **Error! Reference source not found.** illustrates the distribution pattern of vertical stress within soil medium in ITI method and embankment installation (without EPS geofoam) when the maximum pressure of 140 kPa is applied at the backfill surface. In the presence of compressible material soil column above the buried structures settles more than the adjacent soil columns, which leads to the development of positive arching and subsequently culvert top wall undergoes smaller values of vertical stress compared to the no EPS condition. Many researchers have experimentally and numerically noted this trend [56, 58].

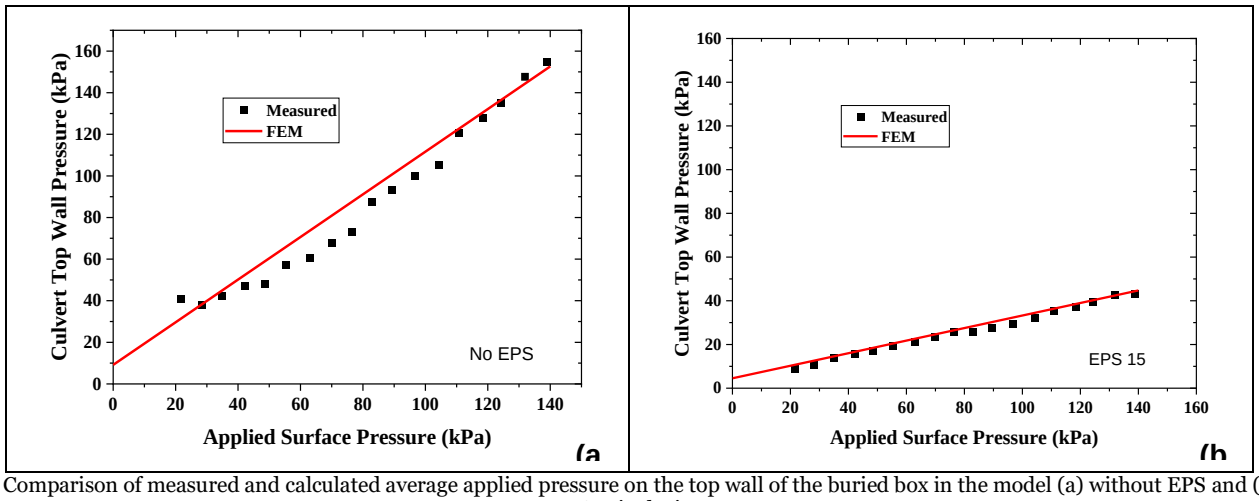

Fig. 2. Comparison of measured and calculated average applied pressure on the top wall of the buried box in the model (a) without EPS and (b) with EPS15 inclusion

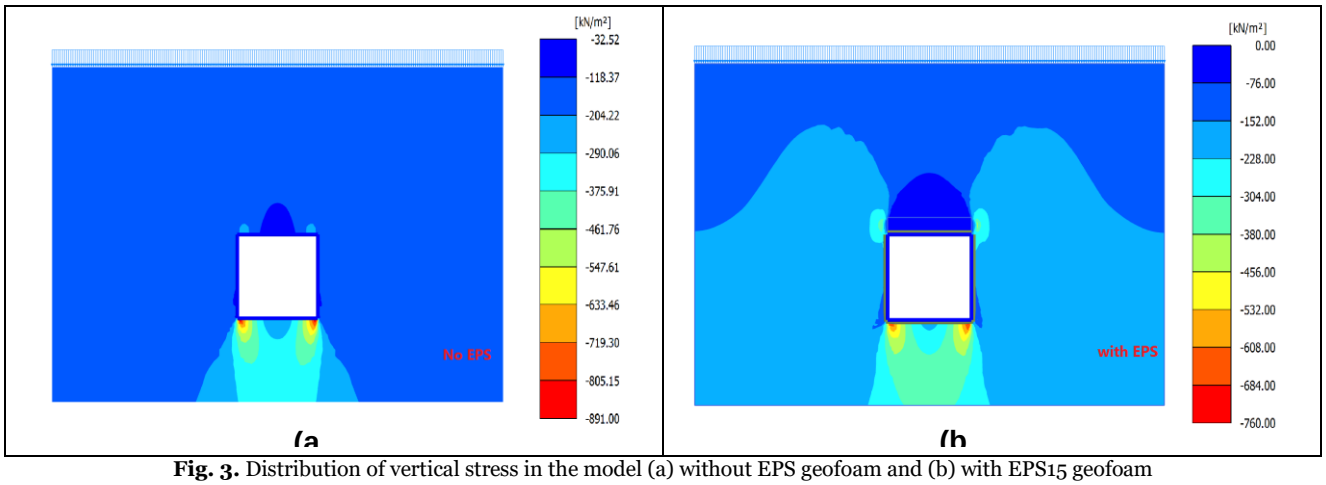

Fig. 3. Distribution of vertical stress in the model (a) without EPS geofoam and (b) with EPS15 geofoam

3.1.Analysis Results and Discussion

Following verification of the numerical model, as discussed in the previous section, a series of two-dimensional finite element analyses have been developed to investigate the effectiveness of three different arrangements of EPS buffer on the performance of buried pipe and ground surface deformation. In the first model, a single block of compressible material is horizontally placed above the pipe (SH Model). Whereas for the second and third arrangements, double blocks will be included horizontally above the pipe (DH Model) and vertically at both sides of the pipe (DV Model). The detailed geometry of each arrangement is shown in Figure 4. The width and thickness of EPS geofoams, respectively, adopted equal to and half of the pipe diameter. The results of No EPS condition will also be presented for a better understanding of the geofoam role in the conducted analysis.

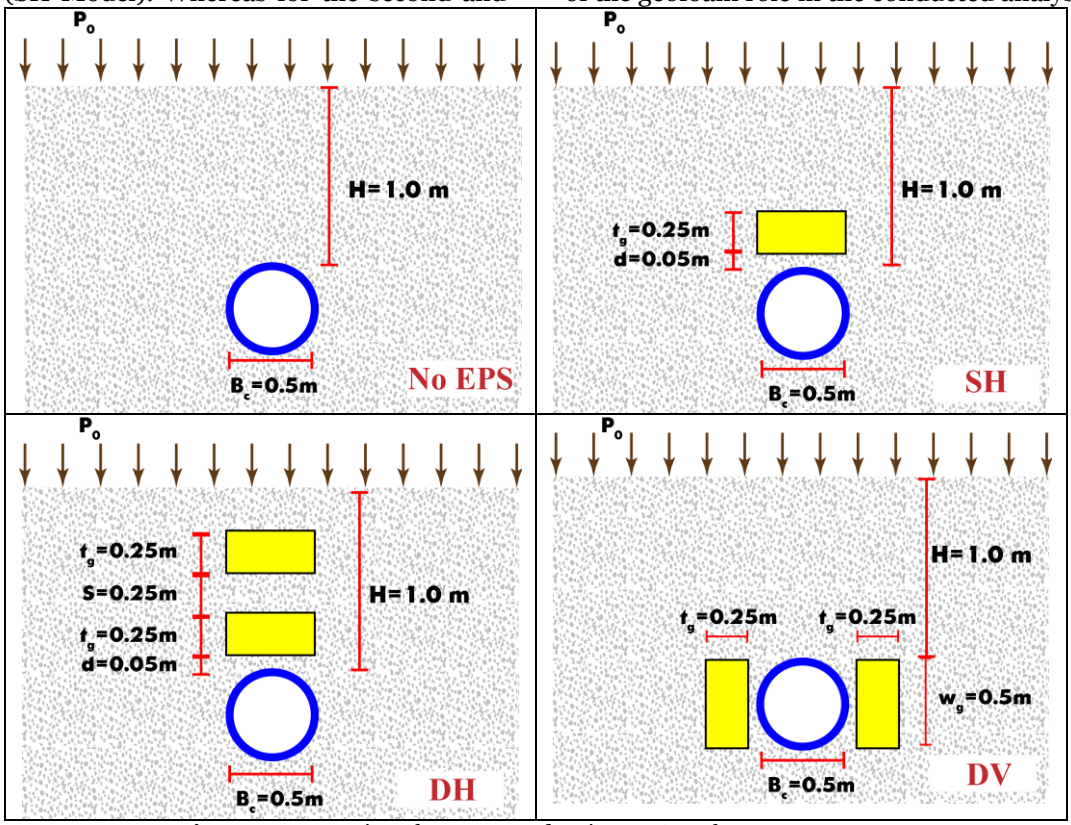

Fig. 4. Representation of geometry and various EPS geofoam arrangements

As the analysis results are intended to be used in a practical situation for a pipeline project in the southern part of Qatar, backfill parameters have been driven from the geotechnical report of the site. Field and laboratory investigations have been performed on the SP sand of the site, the results of which are listed in Table 1. Although the soil cohesion obtained in the laboratory was reported as zero, for numerical stability the negligible value of 1 kPa is introduced to the software. The 5 mm thick pipe behaves linearly elastic with elastic modulus, poisson's ratio, and density of 200 GPa, 0.3, and 7850 kg/m3, respectively. These properties were extracted from product catalogue which was used in the site.

For EPS geofoam, the stiffness of materials is correlated with density. Several studies aimed to propose a relationship between elastic modulus and density of EPS geofoam, which the outcome could be found in the literature [21, 59, 60]. Linear elastic modulus of geofoam buffers used in the numerical analyses of this section was obtained regarding eq.1 suggested by Elragi et al. [59] which presents soil modulus in MPa based on the geofoam density in kg/m3. In this regard, for EPS10, EPS20, and EPS30, values of geofoam modulus are defined as 1.3, 5.4, and 9.5 MPa, whereas the constant value of 0.1 was used as poison's ratio for the three adopted densities.

Table 1. Mechanical properties of backfill soil.

Parameter	Elastic Modulus, E_s (MPa)	Poisson's Ratio (ν)	Cohesion, C (kPa)	Internal Friction Anngle, φ (degree)	Dilation Angle, ψ (degree)
Value	32	0.32	1	33	3

$$E = 0.41\rho - 2.8 \quad (1)$$

Figure 5 illustrates the meshing pattern of the numerical model along with boundary conditions and geometry dimensions. The pipe and EPS inclusions meshes were refined to present sufficient accuracy within the interested zone. The optimum mesh size was adopted through sensitivity analyses by changing element sizes, monitoring the sensitivity of obtained results and uniformity of deformations and stresses around the buried structure, and considering the cost of analyses. The boundaries were chosen far enough from the studied area to avoid the adverse effect of boundaries on the stress and deformation pattern of the soil medium. The ultimate model comprises 3134 elements with variable sizes, finer elements around the pipe, and compressible materials that become larger towards the bottom and side boundaries. Side boundaries are allowed to deform freely in the vertical direction, while the bottom boundary is restrained in the horizontal and vertical directions.

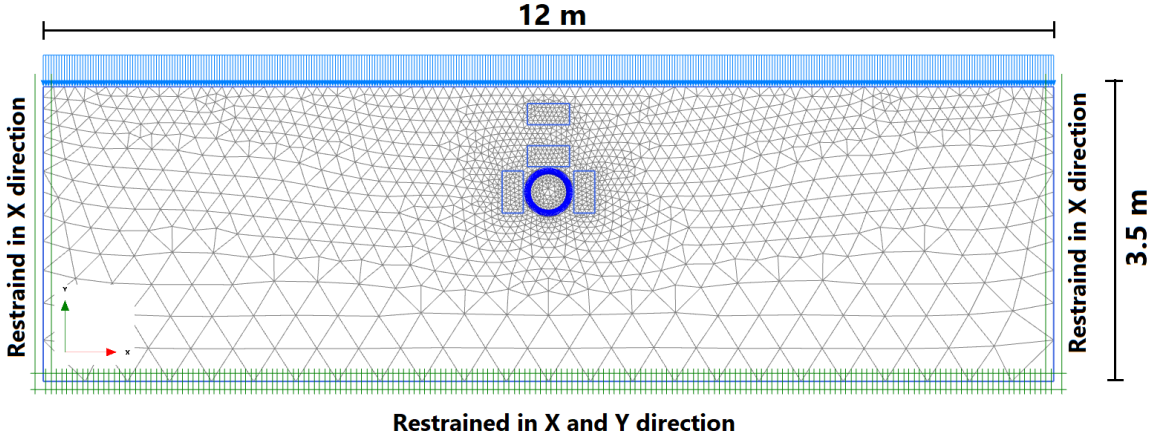

Fig. 5. FE meshing of the model

The numerical modeling is performed using the construction stage technique in which the base layer elements with a thickness of 3 m are first activated. Following that the pipe is installed and later backfill soil layer elements are activated to reach the elevation of EPS material. After placing the geofoam inclusion, backfilling continues to the second EPS (in case of double EPS arrangement) and ultimately to the ground surface. After completion of backfilling, the developed deformation in the model will be reset and surface pressure incrementally increases up to 500 kPa to simulate embankment pressure. In the model with double EPS vertically arranged (DV) adjacent to the pipe, the pipe and compressible zone are simultaneously activated after the activation of base layer elements.

3.2 Surface Settlement

The effect of various geofoam arrangements regarding the stiffness of compressible materials is presented for this part of the study. Figure 6 depicts the ground settlement profile of each configuration for different geofoam densities. As shown, application of the most compressible geofoam buffer (EPS10) leads to the greatest settlement. The maximum settlement is noted above the pipe axis with approximately 94 mm, which is more than 40 mm greater than the maximum settlement in the SH model. Whereas, when no geofoam block is included, the ground settlement profile is almost uniform with no recognizable peak value. In this case, ground vertical deformation is about 43 mm above the pipe axis, while the difference is less than 1 mm for further distances. The surface settlement in this case is due to the pipe deformation as a result of its flexibility. By the provision of double EPS geofoam vertically placed adjacent to the pipe (DV), the maximum settlement reduces compared to the other two cases; however, the region of surface settlement is extended and creates a larger settlement among all studied cases. For instance, at a distance of 1 m from the pipe axis, the computed settlements for No EPS, SH, DH, and DV models are equal to 42.9, 44.6, 44.7, and 48 mm, respectively. Looking at the settlement profiles, it is clear that by moving away from the pipe axis, the differences declined and the value of settlements become close together. For models with EPS10, EPS20 and EPS30, the equal surface settlement location could roughly be noted as 2.6, 2.2 and 1.8 m (measured from pipe axis location).

Variation of peak settlement for models with different geofoam densities has been plotted in Figure 7. It is shown that the max settlement reduces by increasing EPS density and, accordingly, EPS stiffness. The declination rate, however, follows a slower pace for higher densities. While

the settlement in the DH model dropped from 96 to 67 mm by increasing geofoam density from 10 to 20 kg/m3, the provision of geofoam with 30 kg/m3 density decreased the maximum settlement just by 6 mm. Maximum settlement induced by inclusion of horizontally arranged single EPS (SH) and vertically arranged double EPS (DV) is almost equal, with the greatest value of about 54 mm for EPS 10 and the lowest of 46 mm for EPS30. Using double blocks of compressible materials above the pipe (DH model) due to the creation of larger settlements has an adverse effect as far as the surface settlement is concerned.

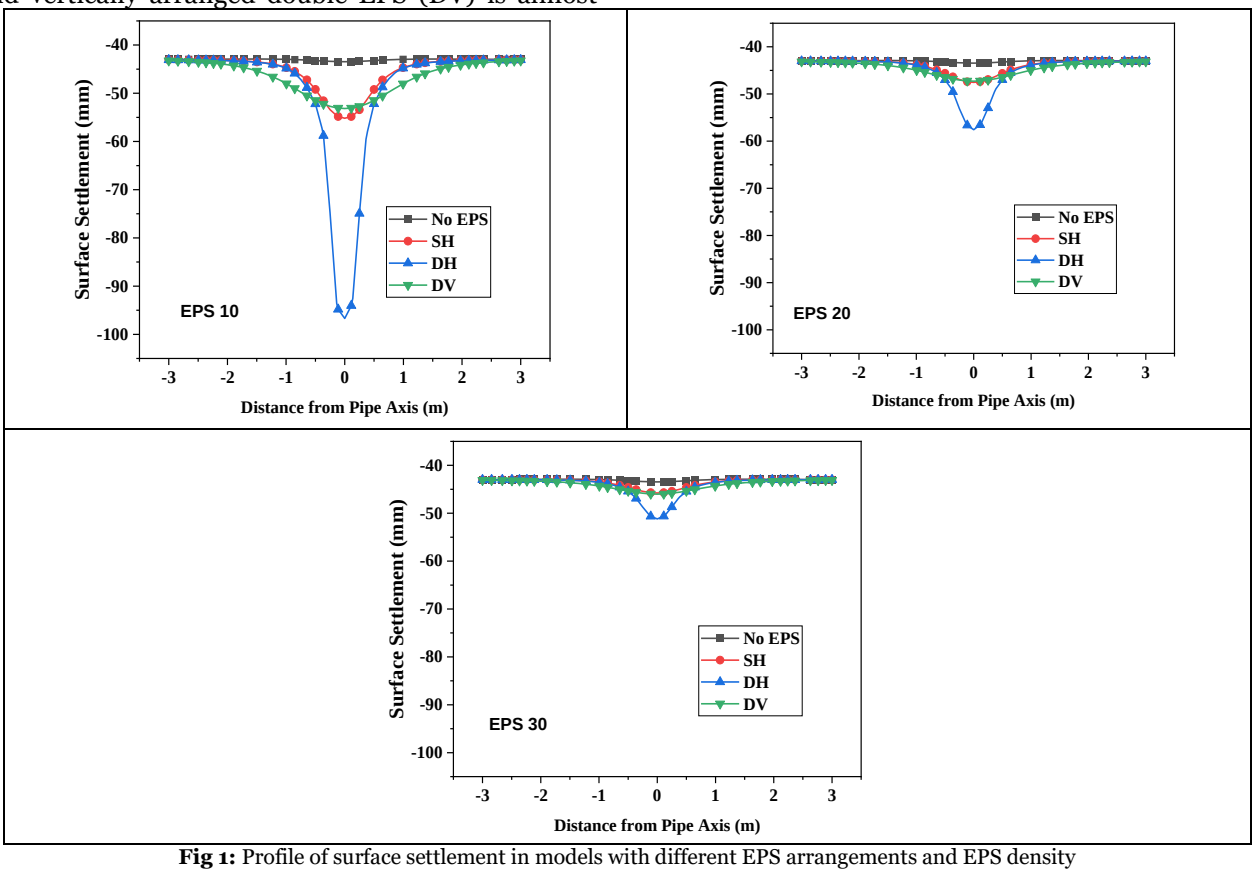

Fig 1: Profile of surface settlement in models with different EPS arrangements and EPS density

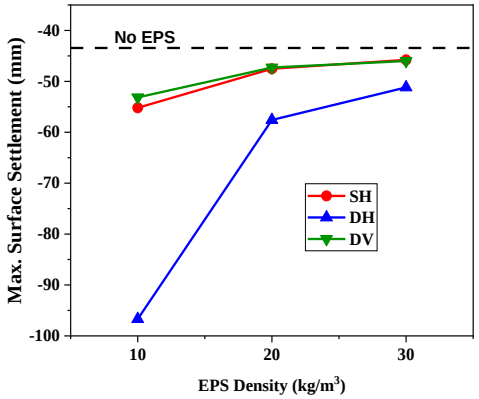

Fig 2: Variation of maximum surface settlement vs. EPS density for different EPS arrangements

3.3. Transferred Pressure to the Buried Pipe

Fig 3 illustrates the vertical stress variation at the crown of the buried pipe versus surface surcharge. This figure shows that transferred pressure to the pipe crest linearly increased with variation in applied surface pressure. Although in the case of DV model with the inclusion of EPS10, buried pipe undergoes more vertical stress compared to the case with no EPS, in models with higher geofoam densities, the differences between models

with and without geofoam buffer are negligible. This gap could be readily observed in Fig 4, where at the ultimate surface pressure of 500 kPa pipe crown bears a pressure just less than 15 kPa (with EPS20 and EPS30) related to the No EPS state. Significant efficiency is noted for models in which geofoam blocks are placed above the pipe, regardless of their number (single or double). Being EPS10 included, applied pressure to the buried pipe was computed equal to 161 and 147 kPa in SH and DH models, respectively. These figures correspond to 33% and 30% of that measured in the model without geofoam buffer. By increasing geofoam density from 10 to 30 kg/m3 the efficiency of buffer decreases. Where the least compressible geofoam (EPS30) is introduced to the SH and DH models, the magnitude of transferred pressure to the pipe crown reaches 391 and 378 kPa (about 80% and 77% of that for no EPS state). Just by considering the crown pressure, it could not be strictly discussed about the efficiency of various arrangements because under embankment load, the distribution of contact pressure around the pipe determines the characteristics of buried pipe design. Thus, the profile of applied pressure to the pipe and developed forces in the pipe skin will be discussed in later sections.

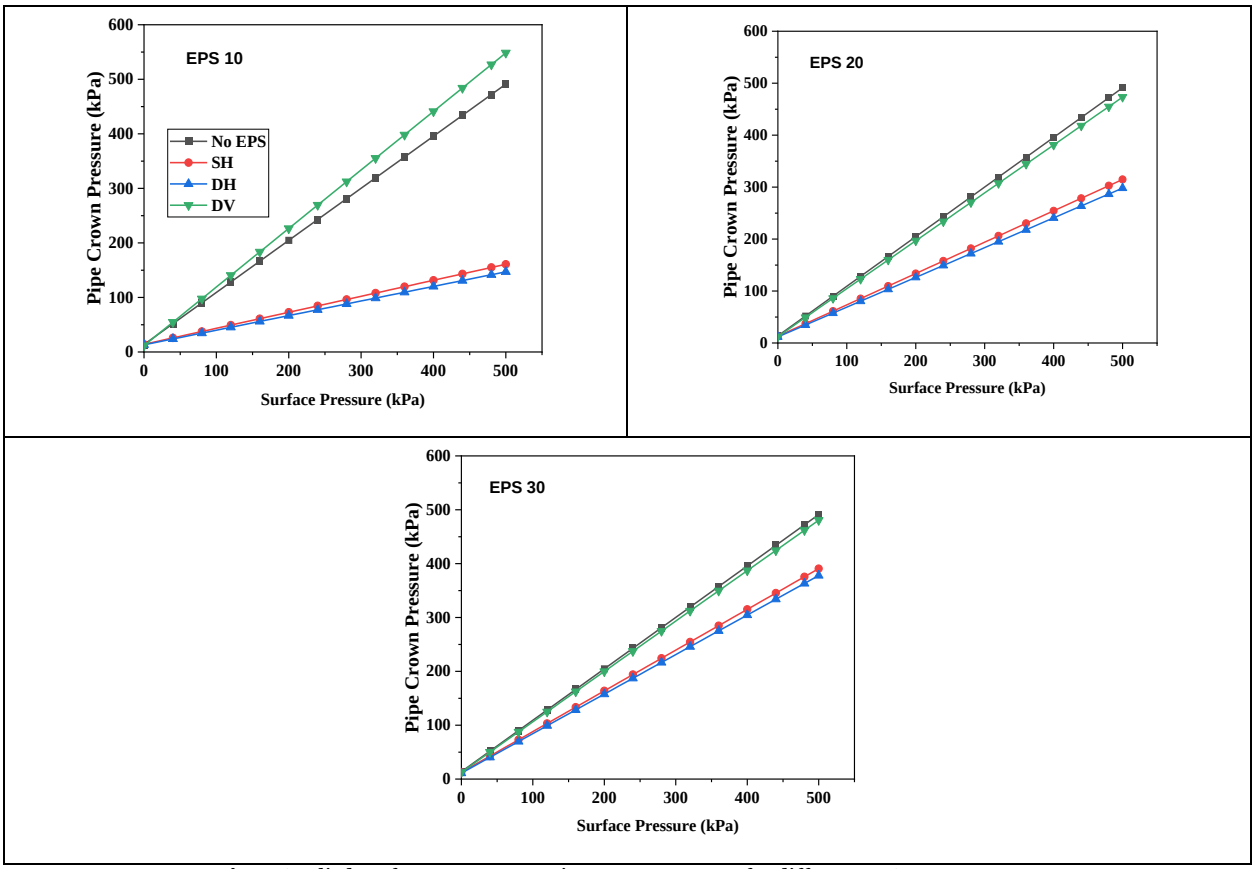

Fig 3: Applied surface pressure vs. pipe crown pressure for different EPS arrangements

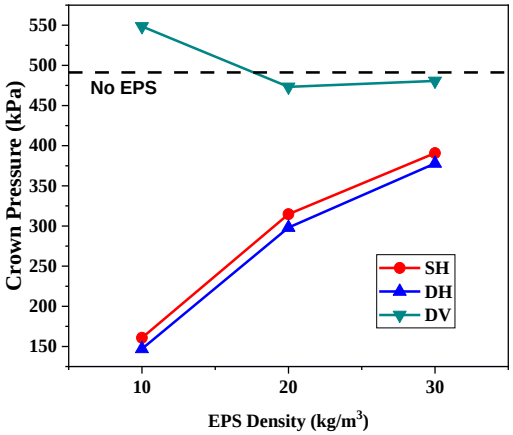

Fig 4: Variation of maximum pipe crown pressure vs. EPS density for different EPS arrangements

3.4. Distribution of Pressure and Deformation

The pattern of transferred pressure along with the pipe deformation for all studied models has been presented in Fig 5. Taking advantage of model symmetry, only responses of one half is depicted. In the figures shown, the right half is attributed to pipe deformation and the other half shows the distribution pattern of normal pressure. A similar pattern of variation can be observed in pipe deformation for all models (with and without geofoam). For all cases, the region between α=0◦ to 90◦ (crown to spring line) depresses related to the undeformed shape, while remained portion bulges to form an oval shape. The maximum values of depression and bulging occur at the crown and spring line. The arrangement of double geofoams adjacent to the structure produces the greatest deformation values, especially in applying the most compressible geofoam (EPS10). This is justified by the fact that due to the lack of horizontal pressure; the pipe crown has more freedom to settlement. In addition, in DV case the crown pressure is greater than in other cases (even greater than no EPS condition) which leads to the formation of a heart shape. The observed sudden changes in case of DV configuration is related to the high compressibility of the EPS geofoam which leads to more deformation toward the buried pipe. However, at the top of vertically arranged EPS blocks there is no soft zone and in that zone the soil mass resist the high deformation of soil. The values of contact pressure at the pipe crown and spring line where the EPS10 is applied, computed equal to 507 and 73 kPa which is far less than the spring line pressure magnitude of 395 kPa in no EPS model. However, by increasing geofoam density to 30 kg/m3 the horizontal thrust of pressure grows to reach the value of 258 kPa, causing more horizontal bearing capacity for the pipe and subsequently less deformation of the pipe crown. Another point worth noting is the development of high-pressure values close to the pipe shoulder and haunch (α=45◦ and 135◦), which is sharply decreased by an increase in geofoam stiffness. The more stiffness is the compressible materials, the more horizontal pressure is exerted on the pipe sides and the less applied at other portions of the pipe circumference.

Overall, the normal pressure experiences by the buried conduit in cases of horizontally placed geofoam blocks (SH and DH) is lower than the magnitude of pressure that the pipe experiences when no geofoam is included. With this regard, the optimum location of compressible material is above the buried pipe provided that the geofoam has sufficient compressibility.

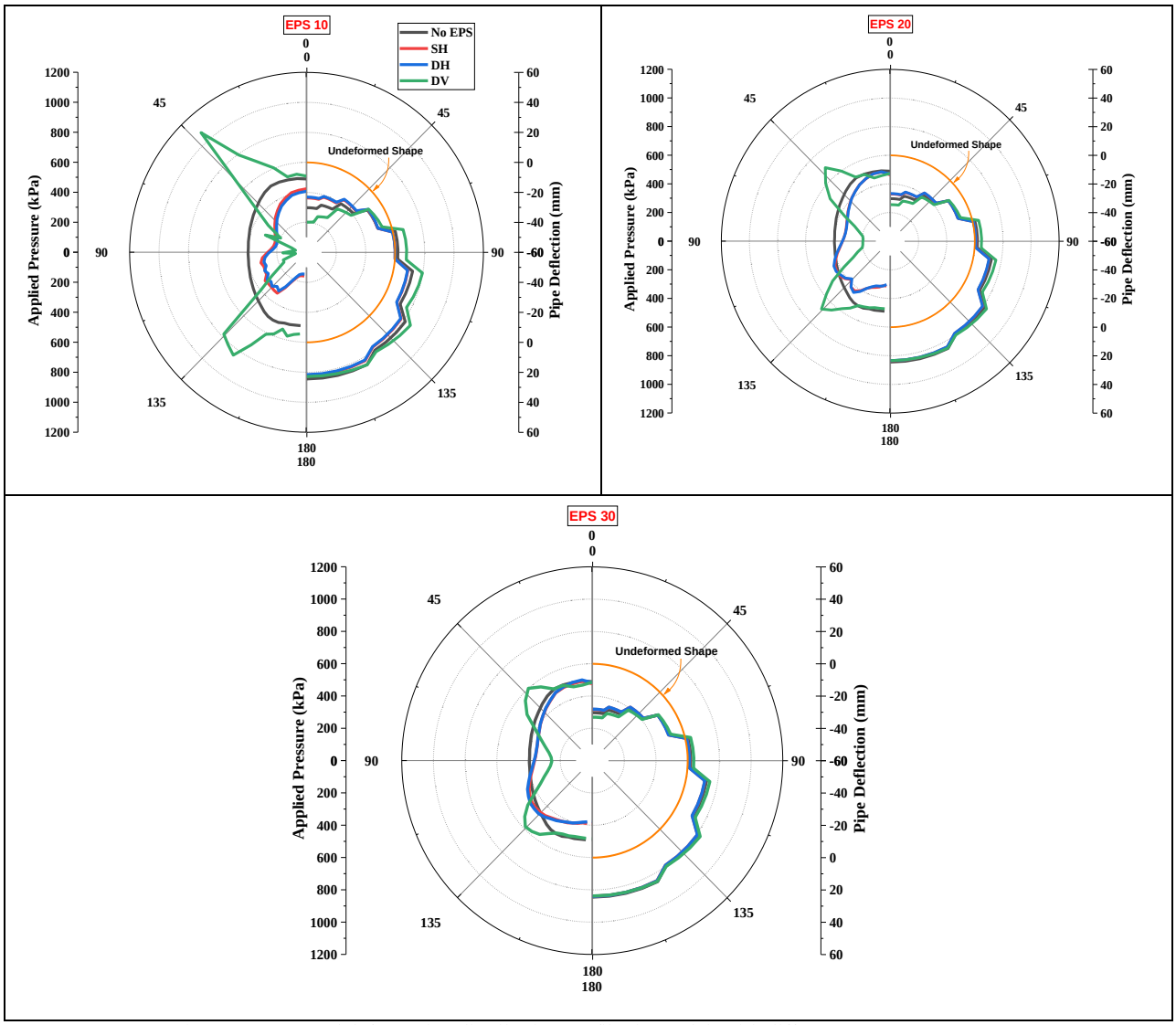

Fig 5: Pressure and deformation distribution profiles in models with different EPS arrangements

3.5. Distribution of Axial and Bending Moments

As the critical factors in designing the pipelines are the mobilized axial and moment bending, this section aims to investigate these parameters in the presence of compressible zones above and beside the buried structure. When compared with no EPS condition, applying geofoam above the buried pipe highly affects the developed forces in the pipe wall (see Fig 6). For SH and DH cases, values of axial forces are less than that in the model with no geofoam buffer. However, the gap becomes smaller with the growth of EPS density as is the case for other pipe responses, including contact pressure and pipe deformation previously discussed. While the pattern of axial forces in SH and DH models is closely matched and the maximum and minimum axial forces develop close to the pipe springline and crown, respectively. By increasing geofoam density from 10 to 30 kPa, crown axial force increases from 57 to 87 kPa and rose from 77 to 124 kPa at the pipe springline (the average of SH and DH models). For the model with vertically arranged geofoams, the mobilized axial force within the crown and springline region is lower and greater than that of in no EPS condition, respectively. Likewise, in the other two models, stiffening the compressible material dictates the pattern and the magnitude of axial forces approaches the no EPS model.

A similar trend can also be observed for mobilized bending moments. As the density of geofoam increases, the efficiency of geofoam inclusion deteriorates and distribution profiles tend to become like the bending moment of unreinforced pipe. The magnitude of developed bending moments at the pipe's crown, springline and invert

are equal to -2.36, +2.44 and -2.36 kN.m. The corresponded value for the case of DH model with EPS10 geofoam buffer, for instance, has been computed as +0.2, +0.6 and -1.2 kN.m which proves a remarkable improvement of pipe performance in the presence of compressible zone. On the other hand, installing geofoam blocks adjacent to the pipe (DV model) adversely affects the pipe response. In this condition, the crown, springline and invert values are changed to -6.65, +8.05 and -6.5 kN.m, which is considerably larger than the values of no EPS state.

In fact, installing geofoam blocks with the same geometry and mechanical characteristics in the wrong direction does not improve pipe behavior and has a detrimental influence that designers should closely notice.

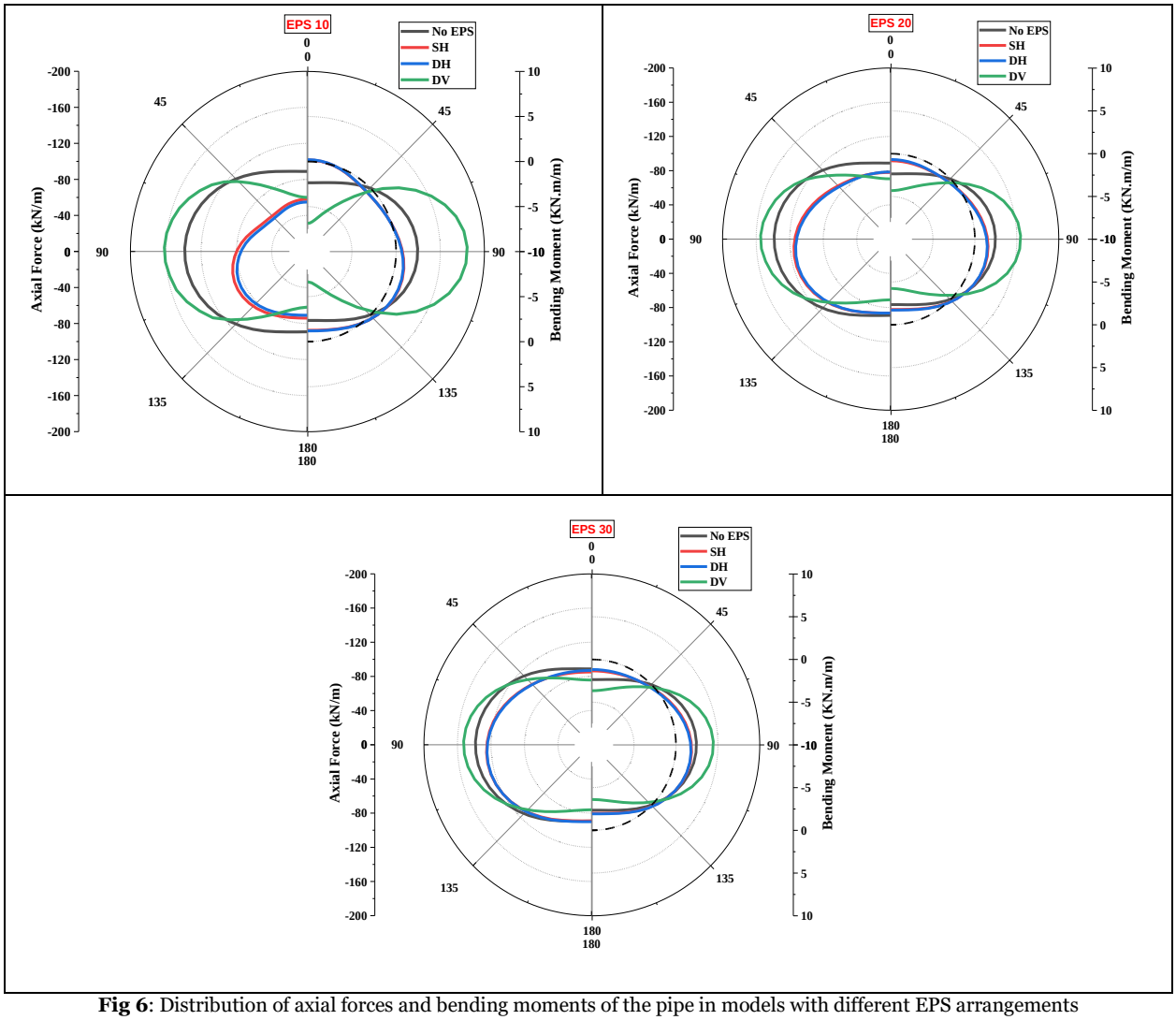

Fig 6: Distribution of axial forces and bending moments of the pipe in models with different EPS arrangements

4.Concluding Remarks

In the present study, the role of various EPS geofoam configurations on the response of pipe buried within sand backfill was investigated by employing two-dimensional numerical analyses. While a large surface pressure has been applied at the surface of backfill sand to simulate height embankment, the transferred pressure to the pipe crest and distribution pattern of axial forces, bending moments, pipe deformation and contact pressure was evaluated. For comparison, the plotted graphs also presented results of a benchmark model in absence of geofoam inclusion. The configuration of EPS buffer was regarded in three forms: (1) a single geofoam block horizontally placed above the pipe (SH Configuration), (2) double geofoam blocks horizontally placed above the pipe (DH Configuration), and (3) double

geofoam blocks vertically installed adjacent to the buried pipe (DV Configuration). The numerical model was initially verified by the measurement of load exerted on a buried structure which had been reported in the literature. From the analysis results and provided charts, the following remarks are summarized:

_ Regardless of the geofoam arrangement type and EPS density, transferred pressure to the buried pipe is linearly increased by the growth of surface pressure. The most significant contact pressure value at the pipe crest could be observed in the model with a double geofoam vertically arranged beside the pipe (DV Model).

_ Inclusion of geofoam blocks above the buried pipe noticeably reduces the earth pressure exerted on the pipe. However, installation of blocks adjacent to the pipe has a detrimental effect on the developed axial forces and bending moments in the pipe wall

_ Using DV configuration is only justified when the reduction of horizontal pressure is regarded as a design requirement.

_ The compressibility of geofoam buffer has a significant effect on the performance of the buried pipe. As the EPS density increases, the pipe response approaches the response of pipe buried in backfill with no geofoam included.

REFERENCES

[1] I. D. Moore and N. A. Hoult, "Performance of two-dimensional analysis: Deteriorated metal culverts under surface live load," Tunnelling and underground space technology, vol. 42, pp. 152-160, 2014.

[2]B. Chen and L. Sun, "The impact of soil properties on the structural integrity of high-fill reinforced concrete culverts," Computers and Geotechnics, vol. 52, pp. 46-53, 2013.

[3]M. Pimentel, P. Costa, C. Félix, and J. Figueiras, "Behavior of reinforced concrete box culverts under high embankments," Journal of Structural Engineering, vol. 135, no. 4, pp. 366-375, 2009.

[4]R. Brachman, T. Elshimi, A. Mak, and I. Moore, "Testing and analysis of a deep-corrugated large-span box culvert prior to burial," Journal of Bridge Engineering, vol. 17, no. 1, pp. 81-88, 2012.

[5]H. Ban, S. Roh, and W.-J. Park, "Performance evaluation of buried concrete pipe considering soil pressure and crack propagation using 3D finite element analysis," Applied Sciences, vol. 11, no. 7, p. 3292, 2021.

[6]J.-H. Yu, H.-G. Wu, C.-Z. Shi, Z. Ma, and W.-T. Xu, "Behavior and innovative design model on soil pressure at the top of large-diameter buried steel pipes," Soils and Foundations, vol. 62, no. 3, p. 101153, 2022.

[7]J. J. Zheng, D. P. Luo, and Q. Ma, "Numerical analysis of slab culvert beneath imperfect ditch covered with geogrid layers," in Applied Mechanics and Materials, 2011, vol. 71: Trans Tech Publ, pp. 3338-3341.

[8]H. El Naggar, A. Turan, and A. Valsangkar, "Earth pressure reduction system using geogrid-reinforced platform bridging for buried utilities," Journal of Geotechnical and Geoenvironmental Engineering, vol. 141, no. 6, p. 04015024, 2015.

[9]A. Dancygier and D. Yankelevsky, "A soft layer to control soil arching above a buried structure," Engineering Structures, vol. 18, no. 5, pp. 378-386, 1996.

[10]N. S. D. Liedberg, "Load reduction on a rigid pipe: pilot study of a soft cushion installation," Transportation research record, vol. 1594, no. 1, pp. 217-223, 1997.

[11]E. Hassankhani, "Applied Pressure on Box Culverts Buried in Rigid Trenches Using Induced Trench Method," Ph.D., Department of Geotechnical Engineering, Tabriz, 2020.

[12]G. Moradi, E. Hassankhani, and A. M. Halabian, "Experimental and numerical analyses of buried box culverts in trenches using geofoam," Proceedings of the Institution of Civil Engineers-Geotechnical Engineering, pp. 1-12, 2020.

[13]A. Marston, "Second progress report to the joint concrete culvert pipe committee," Iowa Engineering Experimental Station, Ames, IA, 1922.

[14]A. Marston, "The theory of external loads on closed conduits in the light of the latest experiments," in Highway research board proceedings, 1930, vol. 9.

[15]G. Moradi, E. Hassankhani, and A. Halabian, "investigation of applied earth load on buried box culverts in trenches using induced trench method under embankment pressure," Sharif Journal of Civil Engineering, vol. 35, no. 4.2, pp. 53-65, 2020..

[16]E. Hassankhani, "Applied Pressure on Box Culverts Buried in Rigid Trenches Using Induced Trench Method," Ph.D., Department of Geotechnical Engineering, University of Tabriz, Tabriz, Iran, 2020.

[17]M. G. Spangler, "Field measurements of the settlement ratios of various highway culverts," 1950.

[18]M. Spangler, "A theory of loads on negative projecting conduits," in Proceedings of the Highway Research Board, 1950, vol. 30: Transportation Research Board Washington (DC), pp. 153-161.

[19]J. Sladen and J. Oswell, "The induced trench method—a critical review and case history," Canadian Geotechnical Journal, vol. 25, no. 3, pp. 541-549, 1988.

[20]J. Horvath, "Expanded polystyrene (EPS) geofoam: an introduction to material behavior," Geotextiles and Geomembranes, vol. 13, no. 4, pp. 263-280, 1994.

[21]J. S. Horvath, "The compressible inclusion function of EPS geofoam," Geotextiles and Geomembranes, vol. 15, no. 1-3, pp. 77-120, 1997.

[22]Z. Li, W. Chen, H. Hao, and M. Z. N. Khan, "Physical and mechanical properties of new lightweight ambient-cured EPS geopolymer composites," Journal of Materials in Civil Engineering, vol. 33, no. 6, p. 04021094, 2021.

[23]M. Esmaeili-Falak, H. Katebi, M. Vadiati, and J. Adamowski, "Predicting triaxial compressive strength and Young's modulus of frozen sand using artificial intelligence

methods," Journal of Cold Regions Engineering, vol. 33, no. 3, p. 04019007, 2019.
[24]M. Esmaeili-Falak and M. Hajialilue-Bonab, "Numerical studying the effects of gradient degree on slope stability analysis using limit equilibrium and finite element methods," Int J Acad Res, vol. 4, no. 4, pp. 216-22, 2012.
[25]R. Sarkhani Benemaran, M. Esmaeili-Falak, and H. Katebi, "Physical and numerical modelling of pile-stabilised saturated layered slopes," Proceedings of the Institution of Civil Engineers-Geotechnical Engineering, pp. 1-16, 2020.
[26]A. Poorjafar, M. Esmaeili-Falak, and H. Katebi, "Pile-soil interaction determined by laterally loaded fixed head pile group," Geomechanics and Engineering, vol. 26, no. 1, pp. 13-25, 2021.
[27]P. Bryden, H. El Naggar, and A. Valsangkar, "Soil-structure interaction of very flexible pipes: centrifuge and numerical investigations," International Journal of Geomechanics, vol. 15, no. 6, p. 04014091, 2015.
[28]O. Abuhajar, H. El Naggar, and T. Newson, "Static soil culvert interaction the effect of box culvert geometric configurations and soil properties," Computers and Geotechnics, vol. 69, pp. 219-235, 2015.
[29]A. Turan, M. H. El Naggar, and D. Dundas, "Investigation of induced trench method using a full scale test embankment," Geotechnical and Geological Engineering, vol. 31, no. 2, pp. 557-568, 2013.
[30]R. P. McAffee and A. J. Valsangkar, "Field performance, centrifuge testing, and numerical modelling of an induced trench installation," Canadian Geotechnical Journal, vol. 45, no. 1, pp. 85-101, 2008.
[31]B. L. McGuigan and A. J. Valsangkar, "Field monitoring and analysis of twin 3660 mm inside diameter induced trench culverts installed under 21.7 m of fill," Canadian Geotechnical Journal, vol. 48, no. 5, pp. 781-794, 2011.
[32]K. YOSHIZAKI and T. Sakanoue, "EXPERIMENTAL STUDY ON SOIL-PIPELINE INTERACTION USING EXPANDED POLYSTYRENE (EPS) BACKFILL," in Pipeline Engineering and Construction International Conference 2003American Society of Civil Engineers, 2003, no. Volume 2.
[33]K. Kim and C. H. Yoo, "Design loading on deeply buried box culverts," Journal of Geotechnical and Geoenvironmental Engineering, vol. 131, no. 1, pp. 20-27, 2005.
[34]J. Kang, F. Parker, and C. H. Yoo, "Soil–structure interaction for deeply buried corrugated steel pipes Part II: Imperfect trench installation," Engineering Structures, vol. 30, no. 3, pp. 588-594, 2008.
[35]L. Sun, T. C. Hopkins, and T. L. Beckham, "Reduction of stresses on buried rigid highway structures using the imperfect ditch method and expanded polysterene (geofoam)," 2009.
[36]L. Sun, T. Hopkins, and T. Beckham, "Load reduction by Geofoam for culvert extension: Numerical analysis," in GeoCongress 2006: Geotechnical Engineering in the Information Technology Age, 2006, pp. 1-5.
[37]X. Qin and Y. Wang, "Reliability-based design of rigid pipes installed by induced trench method with tire-derived aggregate inclusions," Computers and Geotechnics, vol. 140, p. 104456, 2021.
[38]A. Naderi, R. Deng, D. Yu, R. Kania, and L. Li, "Pipe Stress and Deflection During an Integrity Dig," in International Pipeline Conference, 2020, vol. 84447: American Society of Mechanical Engineers, p. V001T03A004.
[39]A. Mohajerani, M. Ashdown, L. Abdihashi, and M. Nazem, "Expanded polystyrene geofoam in pavement construction," Construction and Building Materials, vol. 157, pp. 438-448, 2017.
[40]C. H. Yoo and J. Kang, "Soil-structure interaction for deeply buried corrugated pvc and steel pipes," Highway Research Center, Auburn University, 2007.
[41]M. Meguid, M. Ahmed, M. Hussein, and Z. Omeman, "Earth pressure distribution on a rigid box covered with U-shaped geofoam wrap," International Journal of Geosynthetics and Ground Engineering, vol. 3, no. 2, pp. 1-14, 2017.
[42]M. Meguid, M. Hussein, M. Ahmed, Z. Omeman, and J. Whalen, "Investigation of soil-geosynthetic-structure interaction associated with induced trench installation," Geotextiles and Geomembranes, vol. 45, no. 4, pp. 320-330, 2017.
[43]Y. Beju and J. Mandal, "Combined use of jute geotextile-EPS geofoam to protect flexible buried pipes: Experimental and numerical studies," International Journal of Geosynthetics and Ground Engineering, vol. 3, no. 4, pp. 1-20, 2017.
[44]M. Abdollahi and S. M. Tafreshi, "Numerical investigation on performance of expanded polystyrene geofoam block in protecting buried lifeline structures," International Journal of Geotechnical and Geological Engineering, vol. 11, no. 9, pp. 770-777, 2017.
[45]J. Kang, F. Parker, and C. H. Yoo, "Soil-structure interaction and imperfect trench installations for deeply buried concrete pipes," Journal of geotechnical and geoenvironmental engineering, vol. 133, no. 3, pp. 277-285, 2007.
[46]G. Mohamed, R. Hegazy, and M. Mohamed, "An investigation on the mechanical behavior of expanded polystyrene (EPS) geofoam under different loading conditions," International Journal of Plastics Technology, vol. 21, no. 1, pp. 123-129, 2017.
[47]Y. Beju and J. Mandal, "Expanded polystyrene (EPS) geofoam: preliminary characteristic evaluation," Procedia engineering, vol. 189, pp. 239-246, 2017.
[48]PLAXIS 2D Connect Edition User's Manual. (2021). Bentley Systems, Netherland.
[49]M. Esmaeili-Falak, "Effect of system's geometry on the stability of frozen wall in excavation of saturated granular soils," Doctoral dissertation, University of Tabriz Tabriz, Iran, 2017.
[50]Plaxis 2D Connect Edition User's manual. (2020). Bentley Systems, The Netherlands.
[51]M. Ahmed, Experimental investigations into the role of geosynthetic inclusions on the earth pressure acting on buried structures. McGill University (Canada), 2016.

[52]M. Meguid and M. o. G. Hussein, "A numerical procedure for the assessment of contact pressures on buried structures overlain by EPS geofoam inclusion," International Journal of Geosynthetics and Ground Engineering, vol. 3, no. 1, pp. 1-14, 2017.
[53]J. Kang, F. Parker, Y. J. Kang, and C. H. Yoo, "Effects of frictional forces acting on sidewalls of buried box culverts," International Journal for Numerical and Analytical Methods in Geomechanics, vol. 32, no. 3, pp. 289-306, 2008.
[54]J. Kang, "Finite element analysis for deeply buried concrete pipes in proposed imperfect trench installations with expanded polystyrene (EPS) foams," Engineering Structures, vol. 189, pp. 286-295, 2019.
[55]O. Abuhajar, T. Newson, and H. El Naggar, "Scaled physical and numerical modelling of static soil pressures on box culverts," Canadian Geotechnical Journal, vol. 52, no. 11, pp. 1637-1648, 2015.
[56]O. S. Oshati, A. J. Valsangkar, and A. B. Schriver, "Earth pressures exerted on an induced trench cast-in-place double-cell rectangular box culvert," Canadian Geotechnical Journal, vol. 49, no. 11, pp. 1267-1284, 2012.
[57]R. McAffee and A. Valsangkar, "Performance of an induced trench installation," Transportation Research Record: Journal of the Transportation Research Board, no. 1936, pp. 230-237, 2005.
[58]C. Bryden, K. Arjomandi, and A. Valsangkar, "Distribution of Earth Pressure on Induced Trench Culverts," International Journal of Geomechanics, vol. 22, no. 6, p. 04022072, 2022.